PHYSICAL REVIEW B VOLUME 52, NUMBER 2 1 JULY 1995-II

Spin-glass-like behavior of the incommensurate composite phase $LaCrS_3$

A. Lafond, A. Meerschaut, and J. Rouxel
Laboratoire de Chimie des Solides, Institut des Matériaux de Nantes, CNRS Université de Nantes, 2 rue de la Houssinière,
44072 Nantes-Cédex 03, France

J. L. Tholence and A. Sulpice
Centre de Recherches sur les Très Basses Températures, laboratoire associé à l'Université Joseph Fourier, CNRS, BP 166,
38042 Grenoble-Cédex 9, France

(Received 31 January 1995)

$(La_{0.95}V_{0.05}S)_{1.19}CrS_2$ (V stands for vacancy, often abbreviated "$LaCrS_3$") belongs to the family of composite misfit layer compounds with a structural formulation $(MX)_{1+x}(TX_2)_m$ [G. A. Wiegers and A. Meerschaut, in *Incommensurate Sandwiched Layered Compounds*, edited by A. Meerschaut (Trans. Tech. Pub., Zurich, 1992)]. Chromium is the only magnetic element and antiferromagnetic interactions ($\theta_p = -390$ K) between chromium atoms [$d(\text{Cr-Cr})_{\text{av}} = 3.435$ Å] are taking place. At low temperatures ($T < 80$ K), the susceptibility is largely dependent of the cooling mode: ZFC (zero field cooled) and FC (field cooled). A great number of measurements were performed: magnetization, thermo- and isothermal remanent magnetization, and ac susceptibility on powder and on a single crystal. They all show that $LaCrS_3$ has complex magnetic properties which are reminiscent of spin-glass behavior. These experimental results are discussed in relation with the crystal structure which shows two peculiarities: the (1) chromium framework is a two-dimensional triangular lattice in which antiferromagnetic coupling leads to a topological frustration; and (2) the structural modulation resulting from the mutual interaction between both sublattices ($|LaS|$ and $|CrS_2|$) leads to J/k coupling constant values ranging from -60 to -10 K, in relation to the d(Cr-Cr) distribution [$3.37 \text{ Å} < d(\text{Cr-Cr}) < 3.48$ Å]. These two structural characteristics (frustration and modulation) can explain the formation of magnetic domains in which magnetic moments are not exactly compensated. The resulting moments of these domains are in interaction and can be frozen in the easy magnetization direction giving this compound a spin-glass-like behavior.

I. INTRODUCTION

$LaCrS_3$ belongs to the family of the *misfit layered compounds* with the general formulation $(MX)_{1+x}(TX_2)_m$ (M =Sn,Pb,Bi,Y, rare earths; T=Ti,V,Cr,Nb,Ta; X=S,Se; $0.08 < x < 0.28$; $m = 1$, 2, or 3). (For a review see Ref. 1.)

Their structure results from an alternated stacking of $|MX|$ and $|TX_2|$ slabs along the **c** axis with the $1{:}m$ sequence. This composite nature is characterized by a set of in-plane parameters (a_1, b_1 for the $|MX|$ part and a_2, b_2 for the $|TX_2|$ part) and a common c out-of-plane parameter. Generally, $b_1 = b_2$ but the a_1 and a_2 parameters are different. The a_1/a_2 ratio is irrational and gives the misfit character to these phases.

Magnetic properties of several LTS_3 compounds (L =lanthanides; T=V,Nb,Ta) have been reported.[2-4] These properties are essentially due to the $|LS|$ part.

Chromium misfit derivatives $LCrS_3$ are composed of two magnetic parts ($|LS|$ and $|CrS_2|$).[5,6] The present compound $LaCrS_3$, for which a preliminary study has already been published,[7] has magnetic behavior only related to the $|CrS_2|$ part (Cr^{3+} ions). We report here a detailed study of the magnetic properties of $LaCrS_3$. In the second part of this paper the magnetic properties are discussed in the light of the modulated character of the structure as earlier determined by Kato.[8]

II. EXPERIMENTAL TECHNIQUES

$LaCrS_3$ is prepared by sulfuration of a mixture of $LaCrO_3 + La_2O_3$ (1/10 ratio) in a H_2S gas flow, at 1300 °C for 4 h in a graphite crucible. This process leads to a powdered $LaCrS_3$ compound. This powder with a small amount of iodine for vapor transport was sealed in a quartz ampoule under vacuum (2×10^{-2} torr) and heated at (1000–950 °C) for one week.

The characterization of the samples is made using several methods: semiquantitative analysis in a scanning electron microscope (SEM), microprobe quantitative analysis, and x-ray diffraction on powders and microcrystals.

The misfit layer compound $LaCrS_3$ has been found to be nonstoichiometric.[9] The nonstoichiometry is caused by lanthanum vacancies, the exact chemical formula therefore being $(La_{0.95}V_{0.05}S)_{1.19}CrS_2$, abbreviated as $LaCrS_3$ in this paper.

Magnetic measurements have been performed with the help of a superconducting quantum interference device (SQUID) magnetometer working between 2 and 300 K in a field range between 0 and 6 T. These measurements have been made on powder ($m \approx 140$ mg) and on a single crystal ($m \approx 0.5$ mg). Zero-field-cooled (ZFC) and field-cooled (FC) measurements have been made following slightly different processes for these two samples.

0163-1829/95/52(2)/1112(8)/$06.00

The powder sample was introduced in the magnetometer at a temperature which corresponds to the paramagnetic regime. It was then cooled in zero field (ZFC) down to the initial temperature at which the magnetic field is applied. The ZFC magnetization was measured for increasing temperatures. The sample was then cooled in the same field (FC) and measurements were again taken with increasing temperature. FC measurements of the single crystal have been taken for decreasing temperatures, which in fact gives the same results as those obtained for increasing temperature (used for the powder sample) since the FC magnetization is close to the equilibrium magnetization in a given field.

In the first ZFC measurements on the powder sample, we observed anomalies probably due to the effect of a rather strong residual field (up to a few tens of Oe); such an effect was canceled in further experiments. Some more magnetic measurements have been performed using a Faraday balance: sample weight$\approx$70 mg, $H=17$ kOe, and $100<T<450$ K. All the data were corrected for core diamagnetism and for the sample-holder contribution.

The dynamics have been studied by ac susceptibility measurements in the field, frequency, and temperature ranges $0.1<H<10$ Oe, $10<f<1000$ Hz, and $5<T<300$ K, on samples weighing about 50 mg. The ac susceptibility χ_{ac} is sensitive to the magnetization with fast relaxation times $\tau<1/f$. It is close to χ_{dc} obtained after zero-field cooling.

A powder neutron-diffraction study has been done in order to detect the possible existence of long-range magnetic order in $\mathrm{LaCrS_3}$ (DMC diffractometer, Laboratory for neutron scattering, ETH-Zürich). Preliminary results show that a magnetic two-dimensional (2D) order seems to exist at low temperatures. However, attempts to analyze the magnetic structure have failed because of the very complicated nature of the diffraction pattern.

III. EXPERIMENTAL RESULTS

Figure 1 gives the thermal dependence of the inverse susceptibility of $\mathrm{LaCrS_3}$ (powder sample) for temperatures between 5 and 450 K. For temperatures above 300 K the susceptibility obeys a Curie-Weiss law,

$$\chi=\frac{N_a\mu_{\mathrm{eff}}^2}{3k(T-\theta)}=\frac{C}{T-\theta}\ .$$

It results in a Curie constant ($C=1.9$ emu K mol^{-1}) very close to the spin-only calculated value $C=N_a g^2 J(J+1)/3k=1.875$ emu K mol^{-1}, and a paramagnetic temperature $\theta=-390$ K. This large negative θ value indicates strong antiferromagnetic interactions. In spite of this large θ value, the paramagnetic regime is reached in the temperature range $T>300$ K. The expected valency states of chromium ($\mathrm{Cr^{3+}}$) and of lanthanum ($\mathrm{La^{3+}}$) are confirmed by the experimental Curie constant C.

The dc susceptibility ($\chi_{\mathrm{dc}}=M/H$) has been obtained from magnetization measurements in the zero-field-cooled and field-cooled modes. Figure 2 gives the thermal dependence of the susceptibility of $\mathrm{LaCrS_3}$ and shows a strong magnetic hysteresis between the ZFC and FC parts. A pronounced maximum is observed for the ZFC curve at $T_g\approx70$ K. The hysteresis disappears above 75 K where the two curves coincide. The difference between the FC and ZFC curves is explained by the blocking of the magnetic moments in a paramagnetic state during the ZFC mode. On the contrary, these moments are aligned parallel to the applied field during the FC mode; this leads to a larger magnetization in that case.

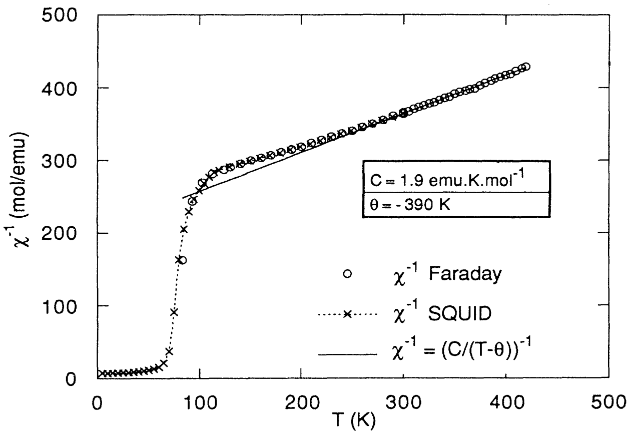

FIG. 1. Thermal dependence of the reciprocal susceptibility (H/M) of $\mathrm{LaCrS_3}$. Measurements were made on compacted powders in an applied field $H=200$ Oe in the SQUID magnetometer and $H=17$ kOe in the Faraday balance.

Figure 3 gives the variation of the magnetic susceptibility of $\mathrm{LaCrS_3}$ for the ZFC and FC conditions, and for various fields (100 Oe, 1 kOe, and 10 kOe). The irreversibility decreases when the field increases and tends to zero for $H>10$ kOe. This corresponds to the fact that the magnetic energy becomes sufficient (in high field) to overcome the energy barrier (or blocking temperature) between the possible equilibrium positions of the magnetic moments. Moreover, the temperature of the maximum of the ZFC curve decreases for increasing fields, which is reminiscent of the behavior of superparamagnets and

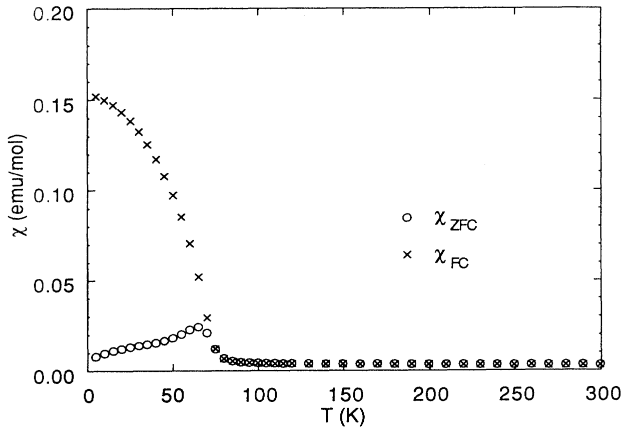

FIG. 2. Thermal dependences of the zero-field-cooled and field-cooled static susceptibility (M/H) of $\mathrm{LaCrS_3}$ (compacted powder).

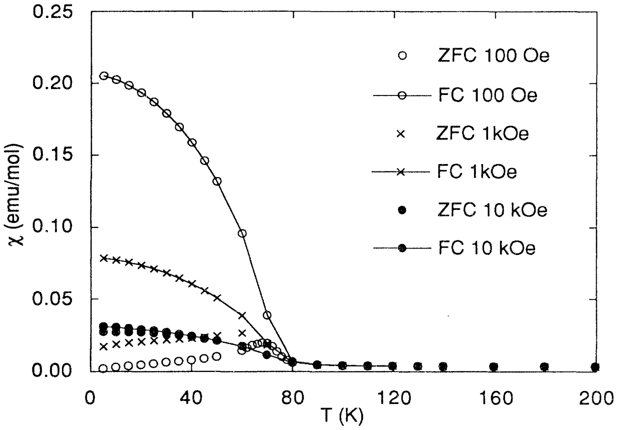

FIG. 3. Comparison of $\chi(T)=(M/H)$ of $LaCrS_3$ (compacted powder) for ZFC and FC conditions in different fields.

spin glasses.

Figure 4 gives the thermal dependence of the dc susceptibility of a single crystal, i.e., respectively, $\mathbf{H}\perp\mathbf{c}(\chi_\perp)$ and $\mathbf{H}\|\mathbf{c}(\chi_\|)$. A strong anisotropy is observed, for $T<80$ K, since a strong irreversibility is observed between the FC and ZFC curves for $\mathbf{H}\perp\mathbf{c}$. Moreover, the susceptibility is much larger along this direction than for $\mathbf{H}\|\mathbf{c}$. The easy direction of magnetization in $LaCrS_3$ is thus parallel to the (a,b) plane as is found for the $LiCrS_2$ compound.[10] The strong anisotropy observed here appears as a general phenomenon for materials with dominant antiferromagnetic interactions. Similarly to what is observed for the powder, the magnetic hysteresis between the FC and ZFC curves of a single crystal decreases for increasing magnetic field, as shown in Fig. 5.

The ac susceptibility has been studied to detect a possible influence of the measuring time on the shape and position of the susceptibility maximum. Figure 6(a) shows the results for several frequencies in a magnetic field of 10 Oe. As expected, these data are similar to those obtained with the SQUID magnetometer in the ZFC mode. The effect of frequency is very weak on the shape and on the position of the susceptibility maximum (T_g). In particular, the time dependence of T_g is much smaller than that expected from the Arrhenius law for superparamagnetic particles. The amplitude of the ac magnetic field ($H\leq 10$ Oe) does not change the result [see Fig. 6(b)].

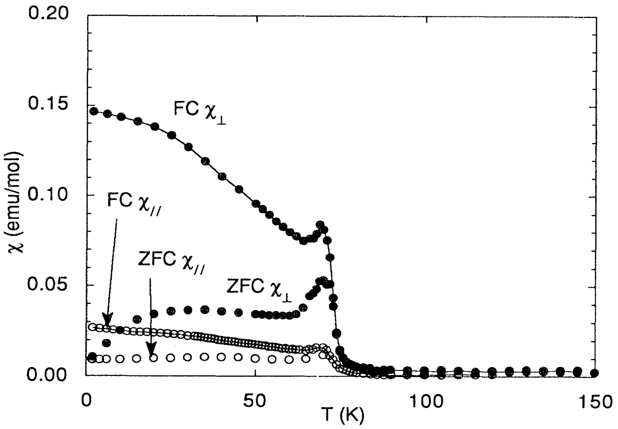

FIG. 4. Temperature dependence of χ for $LaCrS_3$. Measurements are made on a single crystal for the two orientations $\mathbf{H}\perp\mathbf{c}(\chi_\perp)$ and $\mathbf{H}\|\mathbf{c}(\chi_\|)$. $H=100$ Oe.

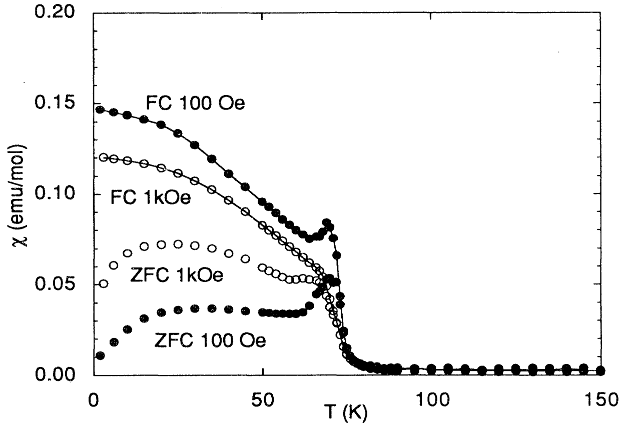

FIG. 5. Thermal dependence of χ for a single crystal of $LaCrS_3$ in a field of 100 Oe and 1 kOe perpendicular to the **c** axis.

The first magnetization curve (after zero-field cooling)

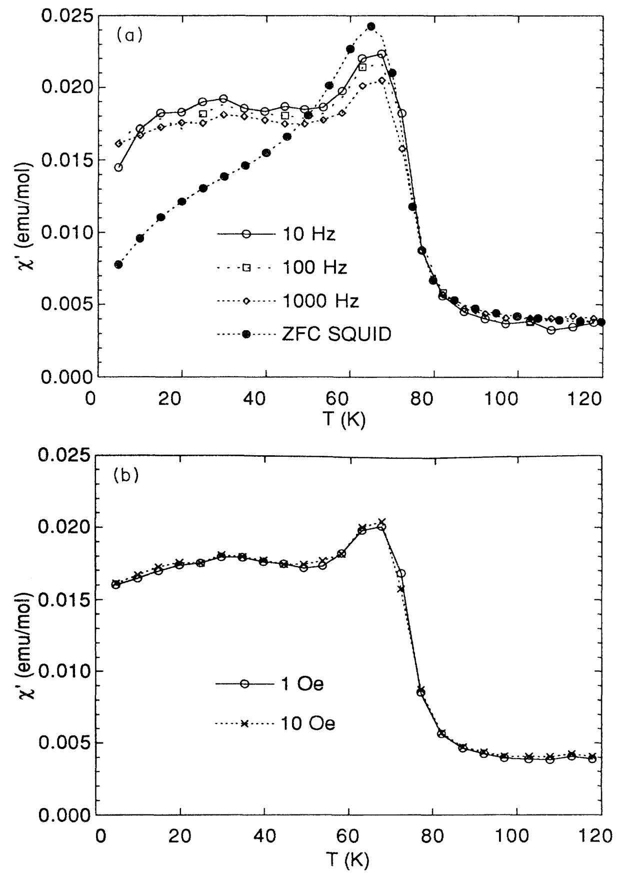

FIG. 6. Thermal dependence of the ac susceptibility of $LaCrS_3$ (compacted powder) for three frequencies and a measuring field of 10 Oe (a) and for two fields at 1000 Hz (b).

of $LaCrS_3$ is shown versus the field increasing from 0 to 50 kOe, at 5 K, in Fig. 7. It is followed by the magnetization obtained in a field decreasing down to zero. From these results we observe the following.

(1) The existence of a remanent magnetization at 5 K.

(2) The saturation has not been reached even in 50 kOe; the magnetic moment in this field corresponds to only 5% of the expected value for all spins ($M = N_a \mu_{Cr^{3+}}$, $\mu_{Cr^{3+}} = \beta g J, g = 2$, and $J = S = \frac{3}{2}$ for Cr^{3+}, which gives $M = 1.67 \times 10^4$ emu/mol). The saturation would be reached in much larger fields.

Depending on the experimental procedure, two different remanent magnetizations can be obtained. Starting from a temperature above the blocking temperature (T_g), and cooling down to $T < T_g$ in a magnetic field, one obtains the thermoremanent magnetization (TRM) when this magnetic field is cut down. For every field and temperature value the whole process has to be repeated (warming above T_g, cooling in a different field value). The other procedure consists of zero-field-cooling the sample from $T > T_g$ down to the temperature T at which the magnetic field is applied for a fixed time (here 300 s), and then switching off to measure the isothermal remanent magnetization (IRM).

Figure 8 gives the thermal dependence of the TRM obtained after cooling in 200 Oe. This remanence starts to appear below 75 K. That temperature range corresponds to the existence of the susceptibility hysteresis. The remanent magnetization increases when the temperature decreases, almost like the magnetization in a constant field.

Both the TRM and IRM depend on the magnetic field applied to the sample, before the measurement in zero field. These dependences are shown in Fig. 9 for $T = 5$ K and $0 < H < 50$ kOe. The TRM increases faster than the IRM in the low-field region and goes through a maximum for a field lower than the field for which the IRM also presents a maximum. Then the TRM and IRM decrease for larger fields. That the TRM is larger than the IRM in low fields is a common characteristic of superparamagnets and spin glasses [see, for instance, AuFe 0.5 at.% (Ref. 11)]. In a general model by Préjean and Souletie,[12] the field necessary to saturate the IRM is two times larger than the field to saturate the TRM. This seems to be the case in our sample too, since the saturations are reached respectively in 7 and 14 kOe for the TRM and IRM. However, the important decrease of these two remanent magnetizations above their saturation field is different from the usual behavior and is not yet explained.

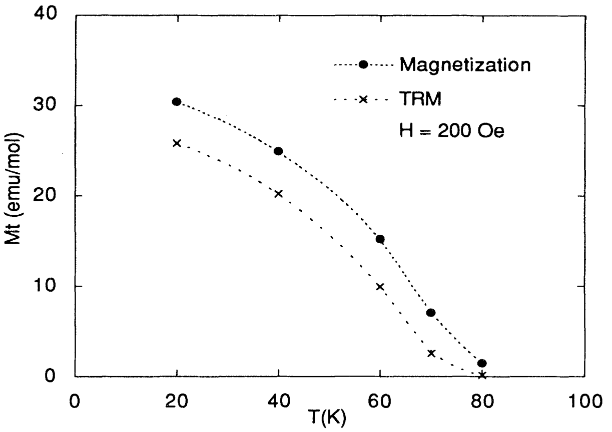

FIG. 8. Thermal dependence of the TRM of $LaCrS_3$ (compacted powder) after cooling in a 200 Oe field applied at 150 K. Dotted lines are guidelines.

IV. DISCUSSION

All these results show that $LaCrS_3$ exhibits a complex magnetic behavior which is reminiscent of a spin glass or a very-small-grained compound. In this part, the magnetic properties are discussed in the light of the modulated character of the structure as early determined by Kato.[8]

A. Description of the structure

Beyond the first approximation of the two independent subsystems (|LaS| and $|CrS_2|$), there exists a mutual

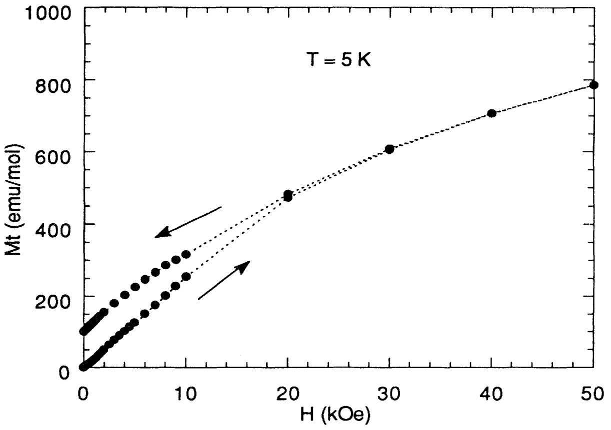

FIG. 7. Field dependence of the magnetization of $LaCrS_3$ (compacted powder) at 5 K after zero-field cooling.

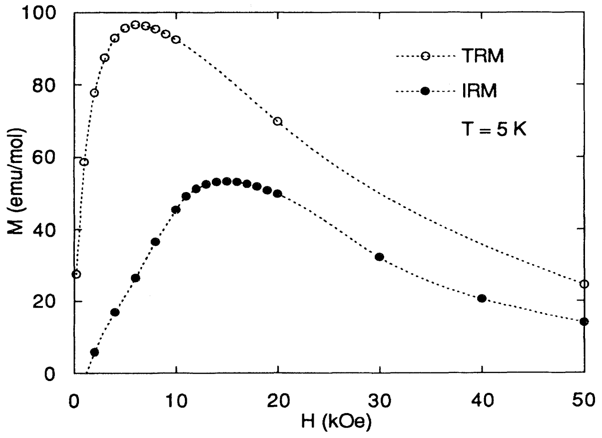

FIG. 9. Field dependence of the TRM and IRM of $LaCrS_3$ (compacted powder) at 5 K.

modulation between the two subsystems. The |LaS| layer is incommensurately modulated with the periodicity of the $|CrS_2|$ layer along the **a** axis and vice versa. Thus the structure of $LaCrS_3$ has been resolved by Kato, in a superspace group.[8] In this approach the modulation due to the interactions between the two sublattices is taken into account. The average structure of this compound (see Fig. 10) is very close to that of other misfits of the $(MS)_{1+x}TS_2$ family. The $|CrS_2|$ part has been described in a triclinic symmetry with positions corresponding to a C lattice mode.

Figure 11 gives the projection of the mean structure of the $|CrS_2|$ sublattice of $LaCrS_3$ in the (a,b) plane. Chromium atoms are octahedrally coordinated by sulfur atoms. Although the cell is triclinic ($\alpha=95.29°$ and $\beta=93.29°$) instead of orthorhombic, the atomic arrangement is comparable to that of $LiCrS_2$,[10] in terms of Cr atomic positions as well as interatomic Cr-Cr distances. Therefore the magnetic interactions between Cr^{3+} might be similar in both lamellar sulfide compounds.

B. Variation of J/k with d(Cr-Cr)

The Kanamori and Goodenough rules[13–15] allow us to predict the type of coupling between transition-metal ions as a function of the geometry of the structure. For a 2D triangular lattice of Cr^{3+} ions ($3d^3$) there exists a competition between the antiferromagnetic (AF) direct coupling Cr-Cr and the superexchange coupling Cr-S-Cr which is ferromagnetic when the two Cr-S bonds make a 90° angle. The importance of the first contribution (AF) increases when the distance Cr-Cr decreases. The resulting interaction [J/k (Ref. 16)] depends on the Cr-Cr distance as shown in Fig. 12 for several sulfide derivatives. In these compounds the $[CrS_6]$ octahedra are edge sharing which means superexchange interactions at 90°.

This dependence of the coupling constant on the nearest-neighbor distances has already been mentioned for other Cr compounds.[20] An extrapolation as a function of the Cr-Cr distance would give a J/k value of the order of -20 K for $LaCrS_3$. In fact, J/k is very sensitive to the Cr-Cr distance since a 4% variation of this distance results in a change from weak ferromagnetism to strong antiferromagnetism as illustrated by $NaCrS_2$ and $Ag_{0.5}Cr_{0.5}PS_3$, respectively.

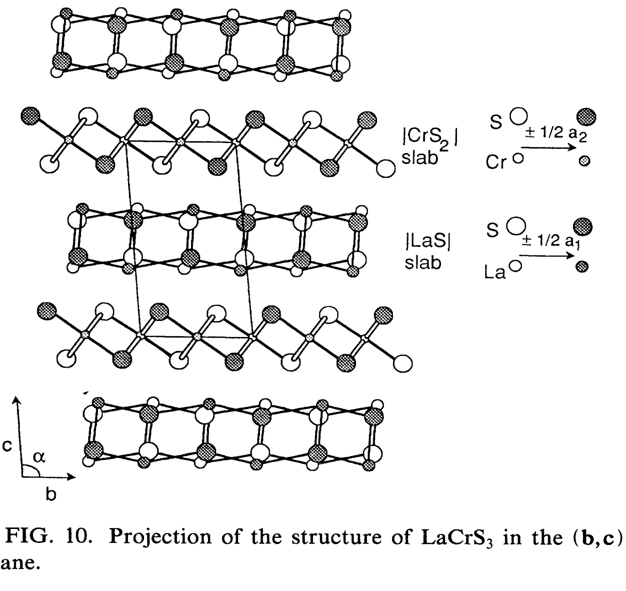

FIG. 10. Projection of the structure of $LaCrS_3$ in the (**b**,**c**) plane.

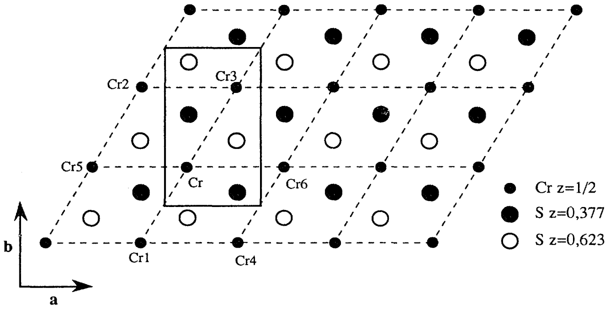

FIG. 11. Projection of the structure of one layer $[CrS_2]$ of $LaCrS_3$ in the (**a**,**b**) plane. For $|CrS_2|$, $a=3.435$ Å, $b=5.936$ Å, $c=11.054$ Å, $\gamma\approx 90°$. This cell is shown in dotted lines on the figure which gives the quasihexagonal structure of the $[CrS_2]$ layer (from Ref. 8).

C. Frustration

Because of the triangular distribution of Cr^{3+} cations, a topological frustration is expected. The large extrapolated θ value (-390 K) means that strong AF interactions exist at room temperature. This feature is well supported by the presence of Cr-Cr distances shorter than those found for $LiCrS_2$. As a consequence, the thermal dependence of the reciprocal susceptibility is not perfectly linear in the 200–300 K temperature range (Fig. 1). In this temperature range, the susceptibility is smaller than that deduced from the Curie-Weiss law. For low-dimensional systems with antiferromagnetic interactions, the $\chi(T)$ curve should exhibit a maximum before the AF transition when the temperature decreases.[21] The absence of such a maximum for $LaCrS_3$ could indicate noncollinear antiferromagnetic interactions in relation to the magnetic frustration.

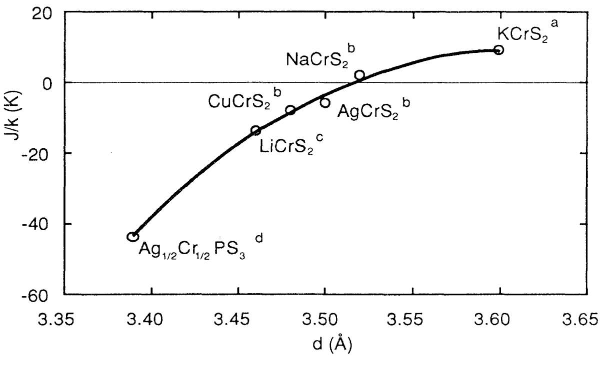

FIG. 12. Relationship between Cr-Cr distance and the magnetic coupling constant ($J_{Cr\text{-}Cr}$). For the reported chromium sulfides, see Refs. 17, 18, 10, and 19, for a, b, c, and d, respectively.

D. Modulation of the Cr-Cr distances

The superspace approach was successfully applied (Kato[8]) to the structure determination of $LaCrS_3$. From these results, the modulation of Cr-Cr distances between a Cr target atom and its six nearest neighbors is calculated (MISTEK program[22]). The variation of each of the six distances, as a function of the modulation's phase t, is thus obtained (see Fig. 13). To be clearer, the graph $d(\text{Cr-Cr}_i)=f(t)$ $(i=1-6)$ indicates every distance occurring between two atoms at any place in an infinite crystal. These interatomic distances range between 3.37 and 3.48 Å. If one assumes that the variation of the exchange integral, as a function of the Cr-Cr distance, is the same as for other sulfide derivatives then the J/k values should range from -78 to -10 K. This means that only antiferromagnetic couplings exist, these ones being more or less important.

The real position of chromium atoms, for a limited assembly of CrS_2 unit cells along the **a** direction, was calculated using the LINE program.[23] Starting from the average structure, the modulation is then introduced [a small shift $(\Delta x, \Delta y, \Delta z)$ of the atomic position]. Related to the misfit character of this structure, only the modulation along the **a** direction is nonperiodic. Thus any translation along **b** or **c** directions gives a corresponding atom which is shifted by the same $(\Delta x, \Delta y, \Delta z)$ vector. Figure 14 shows the modulated distribution of Cr atoms in an array of $40a \times 5b$ of CrS_2 where only the shortest distances are connected. Ribbonlike domains are separated by zones (↑) where the Cr-Cr distances are larger, thus leading to smaller $|J|/k$ values. These domains are perpendicular to the misfit direction (**a**).

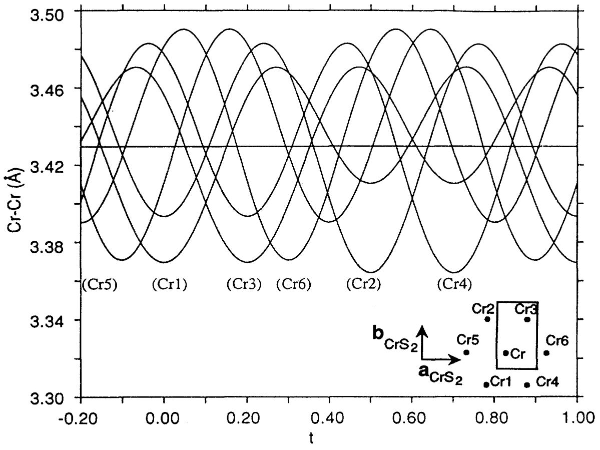

FIG. 13. Variation of the distances between Cr-Cr near-neighbor atoms.

E. Relation between structure and magnetic properties

The $LaCrS_3$ compound is expected to exhibit a spin-glass behavior due to the topological frustration associated with the triangular arrangement of antiferromagnetically coupled Cr^{3+} ions. For such a two-dimensional lattice, the strongest frustration is observed when moments are all aligned along only one direction (Ising spins). In contrast, the system can reach a lower energy in the case of isotropic antiferromagnetic interactions (Heisenberg spins). This is the case for $LiCrS_2$ where the equilibrium corresponds to an orientation at 120° of the magnetic moments in the CrS_2 planes. This example shows that the topological frustration is not sufficient to induce a spin-glass behavior. Toulouse[24] has shown that for spin glasses topological frustration and disorder coexist. However, there is no obvious reason for disorder in $LaCrS_3$.

Results of static susceptibility measurements are characteristic of two types of interactions. Antiferromagnetic interactions which dominate at high temperature are responsible for the large extrapolated negative Curie-Weiss temperature. At temperatures lower than 75 K, the strong increase of the field-cooled magnetization (or susceptibility) is due to an increasing influence of ferromagnetic interactions. Several models[25] could explain the magnetic behavior of $LaCrS_3$.

(a) If there is a random mixture of ferromagnetic and antiferromagnetic interactions, there can be a spin-glass phase at low temperature.

(b) Since the antiferromagnetic interactions dominate at high temperature, one can also assume the existence of antiferromagnetic domains with uncompensated moments (size or edge effects, disorder, etc.). These moments can be frozen below a blocking temperature at which their relaxation time (τ) corresponds to the measuring time $(t=1/f$ in ac susceptibility measurements). Although there is a distribution of blocking temperatures, the irreversibility appears below a peak, at T_g,

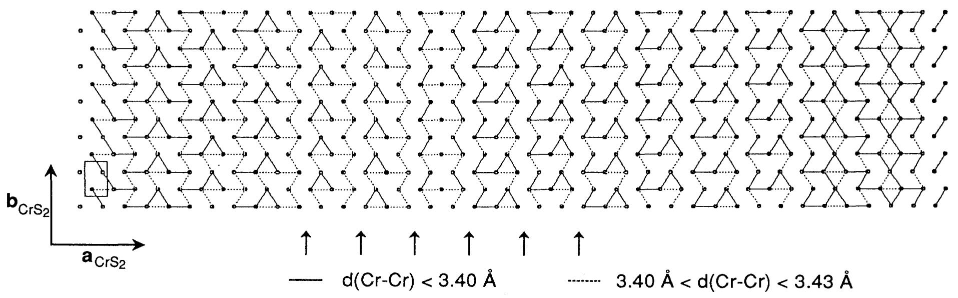

FIG. 14. Representation of the shortest Cr-Cr distances in a $[CrS_2]$ plane of $LaCrS_3$. The atomic positions of Cr are calculated taking into account the structure modulation. The direction of the incommensurability is a_{CrS_2}.

in the ZFC magnetization measured in a low field or in the ac susceptibility. Depending on the interactions between the magnetic moments, T_g can be strongly (weak interactions) or weakly (strong interactions) dependent on the measuring time. In the case of weak interactions a thermally activated regime is observed with a relaxation time described by the Arrhenius law

$$\tau=\tau_0\exp(W/kT) \quad \text{with } \tau_0\approx 10^{-13}\ s \ .$$

Then, T_g is obtained for $\tau=t$,

$$t=1/f=\tau_0\exp(W/kT_g) \ .$$

This corresponds to a strong dependence of T_g on the measuring frequency in ac susceptibility measurements.

In the case of strong interactions T_g will obey a Vogel-Fulcher law

$$\tau=t=1/f=\tau_0\exp[W/k(T_g-T_0)]$$

or a power law $\tau=\tau_0[T_g/(T_g-T_c)]^{z\nu}$, characterized by a weak frequency dependence of T_g. For a canonical spin glass, the relative variation $\Delta T_g/[T_g\Delta\log_{10}(f)]$ per decade of frequency is smaller than 0.06, and the exponent $z\nu$ is of the order of 7 in the power law, which corresponds to T_0 close to T_g in the Vogel-Fulcher law.

Considering the very weak frequency dependence of $T_g(f)$ in $LaCrS_3$ (no change being detected in our limited frequency range), we can conclude that antiferromagnetic domains are in strong interaction. This interpretation is also consistent with the antiferromagnetic Cr-Cr couplings (at high temperature) and the possible effect of a structural modulation on the formation of these domains (which interact ferromagnetically at lower temperatures, close to T_g). The existence of a local antiferromagnetic order has been confirmed by neutron-scattering experiments. The coherence length of the order of a few hundred angstroms would be the average size of our antiferromagnetic domains.

A sharp maximum in the IRM and TRM versus H curves has been observed for the remanent magnetization of $LaCrS_3$. The TRM curves of many spin glasses or superparamagnetic systems also present a small maximum which is still not explained. However, two propositions can be put forward.

(i) Such behavior could result, in terms of magnetic domains, from a rearrangement of some resulting moments in the demagnetizing field created by other magnetic moments aligned in the external field ($H>7$ kOe).

(ii) Another possibility could be that the range of the antiferromagnetic order is extended after applying a large enough external field ($H>7$ kOe) giving then a smaller resulting remanent magnetization.

Other explanations assuming a faster relaxation rate for the remanence obtained in large fields do not seem to apply in our case since we do not observe important changes in this relaxation.

We have a satisfying description of the magnetic properties of $LaCrS_3$ which gives a negligible role to the LaS layers; this means that lanthanum is formally La^{3+} in these layers. The presence of about 5% of La vacancies in the |LaS| subsystem $[(La_{0.95}V_{0.05}S)_{1.19}CrS_2]$ leads to an exact charge balance between La^{3+}, Cr^{3+}, and S^{2-} ions.

V. CONCLUSION

We can conclude that the magnetic properties of $LaCrS_3$ are the result of both a topological frustration and the modulation of the incommensurate structure. Although the magnetic structure could not be determined from neutron-diffraction experiments, we can assume that no long-range magnetic order exist along the *a* direction. But the presence of additional diffracted lines in the low-temperature neutron-diffraction pattern could be due to short-range ordering of the magnetic moments in planes perpendicular to this direction. A description in terms of small two-dimensional antiferromagnetic domains in these planes, with weaker ferromagnetic interactions between their resulting moments, is consistent with all the neutron-diffraction and magnetic measurements.

This is one of the first examples of misfit layer compounds where a close relationship between the modulated structural character and the physical properties is clearly evidenced.

ACKNOWLEDGMENTS

We thank P. Fischer (DMC diffractometer, laboratory for neutron scattering, ETH-Zürich, Switzerland) and H. Mutka (Institut Laue Langevin, Grenoble-France) for the neutron investigation and their fruitful discussions about the magnetic behavior of $LaCrS_3$.

---

[1] G. A. Wiegers and A. Meerschaut, in *Incommensurate Sandwiched Layered Compounds,* edited by A. Meerschaut (Trans. Tech, Zürich, 1991).

[2] O. Peña, P. Rabu, and A. Meerschaut, J. Phys. Condens. Matter **3**, 9929 (1991).

[3] T. Terashima and N. Kojima, J. Phys. Soc. Jpn. **61**, 3303 (1992).

[4] K. Suzuki, N. Kojima, T. Ban, and I. Sujikawa, J. Phys. Soc. Jpn. **59**, 266 (1990); K. Suzuki, T. Enoki, and K. Imaeda, Solid State Commun. **78**, 73 (1991); K. Suzuki, T. Kondo, T. Enoki, and S. Bandow, Synth. Met. **55-57**, 1741 (1993).

[5] A. Lafond, Ph.D. thesis, Nantes University, 1994.

[6] K. Suzuki, T. Kondo, M. Iwasaki, and T. Enoki, Jpn. J. Appl. Phys. **32**, Suppl. 32-3, 341 (1993).

[7] A. Lafond, P. Molinié, A. Sulpice, J.-L. Tholence, A. Meerschaut, and P. Monceau, C. R. Acad. Sci. Ser. II **315**, 1667 (1992).

[8] K. Kato, Acta Crystallogr. Sect. B **46**, 39 (1990).

[9] J. Rouxel, Y. Moëlo, A. Lafond, F. J. DiSalvo, A. Meerschaut, and R. Roesky, Inorg. Chem. **33**, 3358 (1994).

[10] B. van Laar and D. J. Ijdo, J. Solid State Chem. **3**, 580 (1971).

[11] J.-L. Tholence and R. Tournier, J. Phys. (Paris) **35**, C4-229 (1974).

[12] J.-J. Préjean and J. Souletie, J. Phys. (Paris) **41**, 1335 (1980).

[13] J. B. Goodenough, Phys. Rev. **100**, 564 (1955).

[14] J. B. Goodenough, J. Phys. Chem. Solids **6**, 287 (1958).

[15] J. Kanamori, J. Phys. Chem. Solids **10**, 87 (1959).

[16] The isotropic Heisenberg Hamiltonian is $-2J\sum_{i>j}\mathbf{S}_i\cdot\mathbf{S}j$ ($S=3/2$).

[17] B. Van Laar and F. M. R. Engelsman, J. Solid State Chem. **6**, 384 (1978).

[18] P. F. Bongers, C. F. Van Bruggen, J. Koopstra, W. P. F. A. M. Omloo, G. A. Wiegers, and F. Jellinek, J. Phys. Chem. Solids **29**, 977 (1968).

[19] P. Colombet, A. Leblanc, M. Danot, and J. Rouxel, Nouv. J. Chim. **7**, 333 (1983).

[20] P. Colombet and L. Trichet, Solid State Commun. **45**, 317 (1983).

[21] R. Navarro, in *Magnetic Properties of Layered Transition Metal Compounds,* edited by L. J. de Jongh (Kluwer, Dordrecht, 1990).

[22] S. van Smaalen, computer code FORTRAN, Laboratory of Chemical Physics, University of Groningen, The Netherlands, 1992.

[23] A. van der Lee, computer, code FORTRAN, Institut des Matériaux de Nantes, University of Nantes, France, 1993.

[24] G. Toulouse, Commun. Phys. **2**, 115 (1977).

[25] L. Néel Ann. Géophys. **5**, 99 (1949); J. Phys. Rad. **11**, 49 (1950); J. Souletie, J. Phys. (Paris) **44**, 1095 (1983); J. L. Tholence (unpublished).